Nuclear equation of state in the MIT bag crystal model for nuclear matter

Qi-Ren Zhang
Center of Theoretical Physics, CCAST (World Laboratory), Beijing, China
and Department of Technical Physics, Peking University, Beijing 100871, China

Huai-Min Liu*
Physics Department, Peking University, Beijing 100871, China
(Received 10 December 1991)

We developed the MIT bag crystal model for nuclear matter in two aspects. First, we proved a $\Delta\mu=4$ selection rule in the harmonic expansion of quark wave function by group theory. It enables us to push the maximum Dirac quantum number κ_m up from 7 to 15, therefore improving our calculation for the energy band and wave functions of quarks. Then, by a multipole expansion of the color fields we calculate the color interaction energy between quarks. These developments enable us to calculate the energy per nucleon in nuclear matter as done previously for a free nucleon. A nuclear equation of state is derived.

PACS number(s): 21.65.+f, 12.40.Aa

I. INTRODUCTION

For considering quark degrees of freedom in nuclei, bag crystal models for nuclear matter have been proposed [1–5]. In the MIT bag crystal model [5], the crystal is defined by periodic boundary conditions instead of the periodic potential field. Place bags regularly in a lattice and cut overlapping parts out. Windows are opened between adjacent bags. The formed crystal is a huge periodically multiconnected MIT bag; quarks move freely in it, except they are perturbed by the color interaction between them and reflected from the wall by the MIT boundary condition. The translational symmetry reduces our work to that in a cell. Because of this symmetry, values of a single-quark wave function at two corresponding points on two opposite windows separated by a basic vector of the Bravias lattice can only differ from each other by a factor of absolute value 1. Denote this factor in direction i by $\exp(\mathbf{i}p_i a_i)$, $i=1$, 2, or 3. a_i is the lattice constant in direction i. The pseudomomentum $\mathbf{p}=(p_1,p_2,p_3)$ of the quark comes in here. For a given pseudomomentum, this requirement is a definite boundary condition for the single-quark wave function on windows of the cell; it is the periodic boundary condition. The combination of this condition and the MIT boundary condition is the complete boundary condition for quark wave functions. The single-quark wave function satisfies the Dirac equation for a free particle inside the bag cell and satisfies the combined boundary condition on its surface. Therefore we may find the energy and the Bloch wave function for a single quark by subjecting the free-particle Dirac wave function to the boundary condition [5].

The cut bag in a cell is not a sphere and the periodic boundary condition is not spherically symmetric either. The energy eigenfunction for a single quark in it should be a harmonic expansion on the basis of angular momentum eigenfunctions. In numerical calculations this expansion has to be truncated. Working with an N-term expansion, we have to solve an eigenvalue problem of an $N\times N$ matrix. The CPU time and the memory needed is proportional to N^2. An elimination of unnecessary terms is desirable. We work with the simple cubic lattice, in which basic vectors are perpendicular to each other and lattice constants $a_1=a_2=a_3=a$. Authors of [5] have found numerically in this case a $\Delta\mu=4$ selection rule for the harmonic expansion of the quark wave function. We prove this selection rule here in Sec. II by group theory. By this rule we pushed the maximum Dirac quantum number κ_m in the truncated harmonic expansion from 7 up to 15, and therefore improved our results in a limited CPU time and memory.

In Sec. III, we consider the color interactions between quarks by perturbation, as done previously for single hadrons [6]. We use the molecular orbit method, in which the zero-order approximation for the many-quark state is a Slater determinant of single-quark states. Of course, if the density is low enough, the energy band approaches a single energy level; the color interaction, though not strong, may cause appreciable configuration mixing, localizing quarks in cells. In this case, the molecular orbit method fails. Fortunately, at the normal nuclear density the energy band is wide [5]. We assume the molecular orbit method is applicable here and derive the nuclear equation of state around the normal nuclear density by this method. Again, the lack of spherical symmetry makes us work with the multipole expansions of currents and fields.

In Sec. IV, we fix model parameters by fitting baryon data only. This is partly because we have nothing to do with mesons in the MIT bag crystal. Moreover, in

*Permanent address: Institute for High Energy Physics, Academia Sinica, Beijing 100039, China.

modern chiral bag models including Skyrmion models, mesons are point particles rather than bags. Their pressure on a bag surface becomes negligible if the bag radius is large enough. A chiral bag approaches an MIT bag in this limit. The radius of a nucleon bag calculated from our parameters is 1.207 fm, larger than that calculated in [6]. One may think MIT bags with our parameters are limits of chiral bags. We completed our calculation for energy per nucleon in the MIT bag crystal by using this set of parameters, and thus derived the nuclear equation of state in this model. Section V is a short discussion.

II. BLOCH WAVE FUNCTION AND ENERGY BAND

We call the cut bag in a cell (Fig. 1) a bag cell. A cut spherical bag cell is characterized by its radius R and the angle θ_0 defined in Fig. 1 characterizing the size of the window. They are related to the lattice constant a by $a=2R\cos\theta_0$. Because of the translational symmetry of the lattice, we need only to solve the problem in a single bag cell.

In the ground-state nuclear matter, we consider positive energy massless u and d quarks only. The Dirac wave function for a free massless quark with positive eigenenergy ϵ may be written in the form

$$\Psi^{\epsilon}_{\mathbf{p}\nu}(r,\theta,\varphi)=\sum_{\kappa\mu} c^{\epsilon}_{\mathbf{p}\nu}(\kappa\mu)\Phi^{\epsilon}_{\kappa\mu}(r,\theta,\varphi)\ , \tag{2.1}$$

in which $\mathbf{p}$ is the pseudomomentum and ν is an appropriate spin quantum number for a particle in crystal. This is a harmonic expansion on the basis of simultaneous eigenfunctions

$$\Phi^{\epsilon}_{\kappa\mu}(r,\theta,\varphi)=A^{\epsilon}_{\kappa}\begin{bmatrix} \mathbf{j}_{l_\kappa}(\epsilon r)\chi_{\kappa\mu}(\theta\varphi) \\ \mathrm{i}\,\mathrm{sgn}(\kappa)\mathbf{j}_{l_{-\kappa}}(\epsilon r)\chi_{-\kappa\mu}(\theta\varphi)\end{bmatrix} \tag{2.2}$$

of energy ϵ, angular momentum $j_\kappa=|\kappa|-\frac{1}{2}$, its z projection μ and parity $(-1)^\kappa\mathrm{sgn}(\kappa)$. $\kappa=\pm1,\pm2,\pm3,\ldots$ is the Dirac quantum number. $l_\kappa=|\kappa|-[1-\mathrm{sgn}(\kappa)]/2$. $\mathbf{j}_l(\xi)$ is a spherical Bessel function of order l. $\chi_{\kappa\mu}(\theta\varphi)$ is a spinor spherical harmonic function. A^{ϵ}_{κ} is an appropriate normalization constant. Subjecting (2.1) to the combined boundary condition we may [5] solve the eigenenergy ϵ as a function of pseudomomentum $\mathbf{p}$, that is the energy band, and solve the set of expansion coefficients $[c^{\epsilon}_{\mathbf{p}\nu}]$ in (2.1), therefore solving the wave function Ψ itself, that is the Bloch wave function. Ψ is normalized in a bag cell.

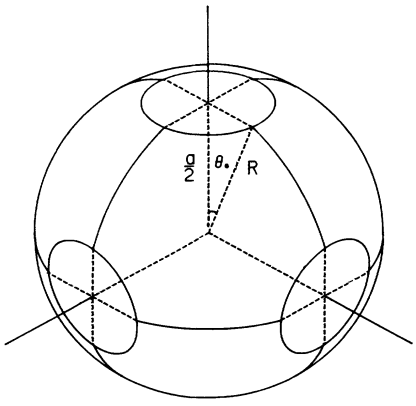

FIG. 1. Cut spherical bag cell in a simple cubic lattice.

A. Selection rule and the reduction of the harmonic expansion

In the numerical calculations we have to truncate the expansion in (2.1) at a maximum absolute value κ_m of κ. To save CPU time and memory, and also to eliminate the accumulative error as much as possible, we would eliminate unnecessary terms from the expansion for a given κ_m. It is the reduction of the expansion. Here we prove the $\Delta\mu=4$ selection rule for the simple cubic lattice. According to this rule, the difference of quantum number μ for two terms in the harmonic expansion of the single-quark wave function is an integer multiple of 4.

Selection rules are from symmetries. Beside the translational symmetry, a lattice also has its point-group symmetry. The point group of a simple cubic lattice is $m3m$ [7]. Euler angles for the 24 rotation elements of this group are

$(0,0,0)$, $(0,0,\pi/2)$, $(0,0,\pi)$, $(0,0,3\pi/2)$,

$(\pi/2,\pi/2,3\pi/2)$, $(3\pi/2,\pi/2,\pi/2)$, $(0,\pi/2,0)$,

$(\pi,\pi/2,\pi)$, $(\pi,\pi/2,0)$, $(0,\pi/2,\pi)$,

$(\pi/2,\pi/2,\pi/2)$, $(3\pi/2,\pi/2,3\pi/2)$, $(\pi/2,\pi/2,0)$,

$(0,\pi/2,\pi/2)$, $(\pi,\pi/2,\pi/2)$, $(\pi/2,\pi/2,\pi)$,

$(0,\pi/2,3\pi/2)$, $(3\pi/2,\pi/2,0)$, $(\pi,\pi/2,3\pi/2)$,

$(3\pi/2,\pi/2,\pi)$, $(3\pi/2,\pi,\pi/2)$, $(0,\pi,0)$, $(\pi,\pi,\pi/2)$,

and $(0,\pi/\pi/2)$.

Substituting these Euler angles in the famous formula (see, for example, [8]) for the irreducible representations $D^{(j_\kappa)}=(D^{(j_\kappa)}_{\mu'\mu})$ of the rotation group, we obtain representations of $m3m$. But they are reducible for $m3m$ in general except the one with $|\kappa|=1$. The irreducibility of $D^{(1/2)}$ for group $m3m$ may be seen by the following reasoning.

$D^{(1/2)}$ is a two-dimensional representation. If it is reducible, there must be a one-dimensional invariant subspace in its representation space. Suppose the only linearly independent spinor in this subspace is

$$\begin{bmatrix} c_1 \\ c_2 \end{bmatrix}.$$

The element

$$D^{(1/2)}(0,\pi,0)=\begin{bmatrix} 0 & -1 \\ 1 & 0 \end{bmatrix}$$

transforms it to

$$\begin{bmatrix} -c_2 \\ c_1 \end{bmatrix}.$$

Invariance of the subspace means $-c_2=bc_1$ and $c_1=bc_2$. The solution of this set of equations is $c_1=\pm ic_2$. On the other hand, the element

$$D^{(1/2)}(0,0,\pi)=\begin{bmatrix}-i & 0\\ 0 & i\end{bmatrix}$$

transforms the same spinor to

$$\begin{bmatrix}-ic_1\\ ic_2\end{bmatrix}.$$

Invariance of the subspace means $-ic_1=b'c_1$ and $ic_2=b'c_2$. The solution of this set of equations is $c_1=0$ and/or $c_2=0$. Therefore we have $c_1=c_2=0$; the supposed invariant subspace is a null space. $D^{(1/2)}$ is an irreducible representation of group $m3m$.

Single-quark wave functions in a free nucleon belong to the $D^{(1/2)}$ representation of the rotation group. By the consideration of correspondence we see the single-quark wave function in a bag cell should belong to the $D^{(1/2)}$ representation of group $m3m$. A projection of $\Phi^{\epsilon}_{\kappa\mu'}$ on the representation space of $D^{(1/2)}$ for $m3m$ is

$$\Phi_\nu=\sum_g\sum_\mu D^{(1/2)}_{\nu\nu'}(g)^* D^{(j_\kappa)}_{\mu\mu'}(g)\Phi^{\epsilon}_{\kappa\mu}$$
$$=\sum_\mu C(\kappa\mu\mu'\nu\nu')\Phi^{\epsilon}_{\kappa\mu}\ , \tag{2.3}$$

g is an element of group $m3m$. ν is the spin quantum number of a quark in a simple cubic lattice, mentioned after (2.1). Completing the summation over g in (2.3), we get

$$C(\kappa\mu\mu'\nu\nu')=\begin{cases}4[\delta_{\nu\nu'}\delta_{\mu\mu'}+(-1)^{|\kappa|+\mu+\nu+1}\delta_{-\mu\mu'}\delta_{-\nu\nu'}]+16S(\kappa\mu\mu')S(1\nu\nu') & \text{if } (\mu-\nu)/2 \text{ and } (\mu'-\nu')/2 \text{ are even},\\ 0 \text{ otherwise},\end{cases} \tag{2.4}$$

with

$$S(\kappa\mu\mu')=\sum_n(-1)^n 2^{-j_\kappa}\frac{\sqrt{(j_\kappa+\mu)!(j_\kappa-\mu)!(j_\kappa+\mu')!(j_\kappa-\mu')!}}{(j_\kappa-\mu-n)!(j_\kappa+\mu'-n)!n!(n+\mu-\mu')!}\ . \tag{2.5}$$

From (2.4) we see, for a given ν, the difference of quantum number μ for two nonzero terms in (2.3), therefore also in (2.1), must be a integer multiple of 4. The selection rule $\Delta\mu=4$ is proven.

This selection rule much reduces the harmonic expansion of the single-quark wave function and makes us be able to push κ_m up from 7 in [5] to 15 here, therefore considerably improving our result. However, the numerical result does not change much compared to that in [5], as it should be.

B. Fourier expansion and the parametrization of the energy band

The factor $\exp(ip_ia_i)$ in the periodic boundary condition itself is a periodic function of p_i, the period is $2\pi/a_i$. Therefore the energy and the Bloch wave function of a single quark are periodic functions of p_i with this period. We may expand $\epsilon(\mathbf{p})$ in a Fourier series of $\mathbf{p}$. The expansion may be further simplified by the point group of the lattice. In the numerical calculations we, of course, have to truncate the series to a finite sum. This is permissible because the contributions to the high harmonic components in this series are from cells far away, therefore they decrease with the period of the harmonic component. This is especially true when we average various quantities over the energy band. A higher harmonic component, with shorter period in $\mathbf{p}$ space, cancels more completely on average. We use the truncated Fourier expansion as an approximate analytic expression of $\epsilon(\mathbf{p})$, with expansion coefficients determined by fitting the numerical results of $\epsilon(\mathbf{p})$ at some specific values of $\mathbf{p}$.

Having considered symmetries for the simple cubic lattice, we suggest the following four-parameter expression for the single-quark energy:

$$\epsilon(\mathbf{p})=\sum_{i=0}^{3}B_i f_i(\mathbf{p})\ , \tag{2.6}$$

with

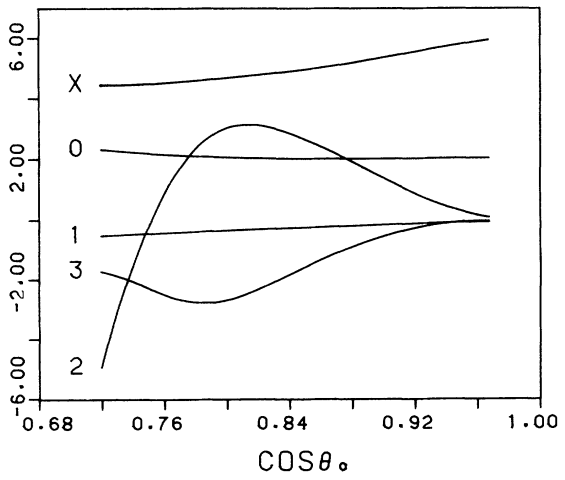

FIG. 2. B_i and E_q as functions of $\cos\theta_0$. Curve i shows RB_i for $i=0,1$, and 10^2RB_i for $i=2,3$. Curve x shows RE_q.

$$
\begin{aligned}
&f_0(\mathbf{p})=1\ ,\\
&f_1(\mathbf{p})=\cos(p_1a)+\cos(p_2a)+\cos(p_3a)\ ,\\
&f_2(\mathbf{p})=\cos(p_1a)\cos(p_2a)+\cos(p_2a)\cos(p_3a)\\
&\qquad+\cos(p_3a)\cos(p_1a)\ ,\\
&f_3(\mathbf{p})=\cos(p_1a)\cos(p_2a)\cos(p_3a)\ .
\end{aligned}
\tag{2.7}
$$

The four parameters B_0, B_1, B_2, and B_3 are determined by fitting four single-quark energies $\epsilon(0,0,0)$, $\epsilon(0,0,\pi/a)$, $\epsilon(\pi/a,\pi/a,0)$, and $\epsilon(\pi/a,\pi/a,\pi/a)$, numerically calculated before. Numerical results for B_i as functions of $\cos\theta_0$ are shown in Fig. 2.

C. Average quark energy per nucleon E_q

For a given pseudomomentum there are two spin states with $\nu=\pm\frac{1}{2}$, two isospin states, and three color states; altogether $2\times2\times3=12$ combinations. Filling quarks into the energy band up to the Fermi energy ϵ_F, we obtain the zero-order approximate state of the quark system according to the molecular orbit method. There is one nucleon per cell, therefore a three-quark per a^3 volume on average. We find

$$
\frac{a^3}{(2\pi)^3}\int\int\int_{-\pi/a}^{\pi/a}F(\mathbf{p})d^3p=3\ ,
\tag{2.8}
$$

with

$$
F(\mathbf{p})=\begin{cases}12 & \text{if } \epsilon(\mathbf{p})\le\epsilon_F\ ,\\ 0 & \text{otherwise}\ .\end{cases}
\tag{2.9}
$$

This condition determines the Fermi energy ϵ_F. Substituting the determined ϵ_F into (2.9), we obtain a well defined occupation function $F(\mathbf{p})$. Using it and the expression (2.6) for $\epsilon(\mathbf{p})$ with the determined parameters B_i, we calculate average quark energy per nucleon

$$
E_q=\frac{a^3}{(2\pi)^3}\int\int\int_{-\pi/a}^{\pi/a}\epsilon(\mathbf{p})F(\mathbf{p})d^3p\ .
\tag{2.10}
$$

The numerical result of E_q as a function of $\cos\theta_0$ is also shown in Fig. 2.

III. COLOR INTERACTIONS BETWEEN QUARKS

In nuclear matter composed of massless u and d quarks only, the color charges cancel completely everywhere, and the color electric energy is zero, just as in a single strangeless hadron. Because of the translational symmetry of the lattice, we need only consider the color magnetic energy per cell $E_{\text{c.m.}}$. The color magnetic interaction is a two-body interaction. Denoting the color magnetic field of octet color k associated with quark i and at position $\mathbf{r}$ by $\mathbf{H}^{(k)}(i,\mathbf{r})$, we have for the state $|\ \rangle$ of the quark system

$$
E_{\text{c.m.}}=-2\pi\alpha_c\int_{\text{cell}}\sum_{i\neq i'}\sum_{k=1}^{8}\langle\,|\mathbf{H}^{(k)}(i,\mathbf{r})\cdot\mathbf{H}^{(k)}(i',\mathbf{r})|\,\rangle d\tau\ ,
\tag{3.1}
$$

where α_c is the color fine-structure constant. According to the molecular orbit method, state $|\ \rangle$ is a determinant of single-quark states $|\iota\rangle$. Therefore

$$
E_{\text{c.m.}}=-2\pi\alpha_c\int_{\text{cell}}\sum_{\iota\iota'}[\langle\iota'|\mathbf{H}^{(k)}(\mathbf{r})|\iota'\rangle\cdot\langle\iota|\mathbf{H}^{(k)}(\mathbf{r})|\iota\rangle-\langle\iota|\mathbf{H}^{(k)}(\mathbf{r})|\iota'\rangle\cdot\langle\iota'|\mathbf{H}^{(k)}(\mathbf{r})|\iota\rangle]d\tau\ .
\tag{3.2}
$$

$\mathbf{H}^{(k)}(\mathbf{r})$ is a color magnetic field associated with a single quark. The single-quark state is a direct product of the space-spin state $|\mathbf{p}\nu\rangle$, the isotopic state $|f\rangle$, and the color state $|c\rangle$. $\Psi^{\epsilon}_{\mathbf{p}\nu}$ in (2.1) is the coordinate representation of $|\mathbf{p}\nu\rangle$. We may also factorize $\mathbf{H}^{(k)}=\mathbf{H}\lambda^{(k)}$, in which $\mathbf{H}$ is color independent and $\lambda^{(k)}$ is the kth generator of the color SU(3) group. Since nuclear matter is colorless, we always sum over complete color triplets in (3.2). Using the fact that the color field operators do not act on flavor state $|f\rangle$, the orthonormality $\langle f|f'\rangle=\delta_{f,f'}$, identities $\sum_{c=1}^{3}\langle c|\lambda^{(k)}|c\rangle\equiv\mathrm{Tr}\lambda^{(k)}=0$, and

$$
\sum_{k=1}^{8}\sum_{c,c'=1}^{3}\langle c|\lambda^{(k)}|c'\rangle\langle c'|\lambda^{(k)}|c\rangle=\sum_{k=1}^{8}\mathrm{Tr}(\lambda^{(k)})^2=16\ ,
\tag{3.3}
$$

we obtain

$$
E_{\text{c.m.}}=\frac{4\pi\alpha_c}{9}\int\int\int_{-\pi/a}^{\pi/a}\frac{a^3d^3p}{(2\pi)^3}F(\mathbf{p})\int\int\int_{-\pi/a}^{\pi/a}\frac{a^3d^3p'}{(2\pi)^3}F(\mathbf{p}')\int_{\text{cell}}\sum_{\nu\nu'}|\langle\mathbf{p}\nu|\mathbf{H}(\mathbf{r})|\mathbf{p}'\nu'\rangle|^2d\tau\ .
\tag{3.4}
$$

The color magnetic field $\mathbf{H}^{(k)}(\mathbf{r})$ satisfies the field equation $\nabla\times\mathbf{H}^{(k)}(\mathbf{r})=\mathbf{I}^{(k)}(\mathbf{r})$, where $\mathbf{I}^{(k)}(\mathbf{r})$ is the color current. We then factorize the color current, $\mathbf{I}^{(k)}(\mathbf{r})=\mathbf{I}(\mathbf{r})\lambda^{(k)}$. $\mathbf{I}(\mathbf{r})$ is a color-independent factor. The field equation becomes $\nabla\times\mathbf{H}(\mathbf{r})=\mathbf{I}(\mathbf{r})$, which is common for every kind of color. Color fields satisfy this field equation in the bag cell, satisfy the MIT boundary condition $\hat{\mathbf{r}}\times\mathbf{H}=0$ on the wall, and the periodic boundary condition on windows. We may think that the field $\mathbf{H}$ in a bag cell is a superposition of two parts, $\mathbf{H}_s$ and $\mathbf{H}_f$. $\mathbf{H}_s$ is the field generated by the current in the bag cell under consideration, therefore satisfies the inhomogeneous field equation $\nabla\times\mathbf{H}_s(\mathbf{r})=\mathbf{I}(\mathbf{r})$ and vanishes at infinity. $\mathbf{H}_f$ is the field generated by currents in other bag cells and the field reflected from the wall, therefore satisfies the sourceless field equation $\nabla\times\mathbf{H}_f(\mathbf{r})=0$ in the bag cell under consideration, and makes the total field $\mathbf{H}=\mathbf{H}_s+\mathbf{H}_f$ satisfy the combined boundary conditions. We solve $\mathbf{H}(\mathbf{r})$ from this well-defined boundary-value problem in the following.

A. Multipole expansion for color currents and fields

From (2.1) we see the matrix element of current

$$\langle \mathbf{p}\nu|\mathbf{I}(\mathbf{r})|\mathbf{p}'\nu'\rangle=\Psi^{\epsilon}_{\mathbf{p}\nu}(\mathbf{r})^{\dagger}\vec{\alpha}\Phi^{\epsilon'}_{\mathbf{p}'\nu'}(\mathbf{r})=\sum_{\kappa\mu\kappa'\mu'}c^{\epsilon}_{\mathbf{p}\nu}(\kappa\mu)^{*}\langle \epsilon\kappa\mu|\mathbf{I}(\mathbf{r})|\epsilon'\kappa'\mu'\rangle c^{\epsilon'}_{\mathbf{p}'\nu'}(\kappa'\mu') , \tag{3.5}$$

with

$$\langle \epsilon\kappa\mu|\mathbf{I}(\mathbf{r})|\epsilon'\kappa'\mu'\rangle=\mathbf{i}\chi_{\kappa\mu}(\theta\varphi)^{\dagger}[u^{\epsilon\epsilon'}_{+}(r)\hat{\mathbf{r}}+\mathbf{i}u^{\epsilon\epsilon'}_{-}(r)\hat{\mathbf{r}}\times\vec{\sigma}]\chi_{\kappa'\mu'}(\theta\varphi) , \tag{3.6}$$

and

$$u^{\epsilon\epsilon'}_{\pm}(r)=A^{\epsilon}_{\kappa}A^{\epsilon'}_{\kappa'}[-\mathrm{sgn}(\kappa')\mathbf{j}_{l_\kappa}(\epsilon r)\mathbf{j}_{l_{-\kappa'}}(\epsilon' r)\pm\mathrm{sgn}(\kappa)\mathbf{j}_{l_{-\kappa}}(\epsilon r)\mathbf{j}_{l_{\kappa'}}(\epsilon' r)] . \tag{3.7}$$

$\vec{\alpha}$ is a Dirac matrix vector, $\vec{\sigma}$ is a Pauli matrix vector, and $\hat{\mathbf{r}}$ is a unit radius vector. A simple Racah algebraic derivation gives (see Appendix A)

$$\chi_{\kappa\mu}(\theta\varphi)^{\dagger}\hat{\mathbf{r}}\chi_{\kappa'\mu'}(\theta\varphi)=\sum_{LJM}X_{LJ}(\kappa\kappa')C^{j_{\kappa'}\mu'}_{j_\kappa\mu J M}\mathbf{T}_{LJM}(\theta\varphi) \tag{3.8}$$

and

$$\chi_{\kappa\mu}(\theta\varphi)^{\dagger}\mathbf{i}(\hat{\mathbf{r}}\times\vec{\sigma})\chi_{\kappa'\mu'}(\theta\varphi)=\sum_{LJM}Y_{LJ}(\kappa\kappa')C^{j_{\kappa'}\mu'}_{j_\kappa\mu J M}\mathbf{T}_{LJM}(\theta\varphi) , \tag{3.9}$$

with

$$X_{LJ}(\kappa\kappa')=\sum_{\kappa_1}(-1)^{J+l_\kappa+\kappa'+\kappa_1+1}\left[\frac{2|\kappa|(2J+1)(2l_\kappa+1)(2l_{\kappa'}+1)(2l_{\kappa_1}+1)}{\pi}\right]^{1/2}|\kappa_1|C^{l_{\kappa_1}0}_{10l_\kappa 0}$$
$$\times C^{L0}_{l_{\kappa_1}0l_{\kappa'}0}\begin{Bmatrix}1 & l_\kappa & l_{\kappa_1}\\ \frac{1}{2} & j_{\kappa_1} & j_\kappa\end{Bmatrix}\begin{Bmatrix}j_{\kappa_1} & l_{\kappa_1} & \frac{1}{2}\\ l_{\kappa'} & j_{\kappa'} & L\end{Bmatrix}\begin{Bmatrix}j_\kappa & 1 & j_{\kappa_1}\\ L & j_{\kappa'} & J\end{Bmatrix} , \tag{3.10}$$

and

$$Y_{LJ}(\kappa\kappa')=\sum_{\kappa_1\kappa_2}(-1)^{J+L+l_\kappa+l_{\kappa'}+\kappa+\kappa_1+\kappa_2+1}12|\kappa_1\kappa_2|\left[\frac{2|\kappa|(2J+1)(2l_\kappa+1)(2l_{\kappa'}+1)(2l_{\kappa_1}+1)}{\pi}\right]^{1/2}$$
$$\times\delta_{l_{\kappa_2}l_{\kappa'}}C^{l_{\kappa_1}0}_{10l_\kappa 0}C^{L0}_{l_{\kappa_1}0l_{\kappa'}0}\begin{Bmatrix}1 & l_\kappa & l_{\kappa_1}\\ \frac{1}{2} & j_{\kappa_1} & j_\kappa\end{Bmatrix}\begin{Bmatrix}j_{\kappa_1} & l_{\kappa_1} & \frac{1}{2}\\ l_{\kappa'} & j_{\kappa_2} & L\end{Bmatrix}\begin{Bmatrix}l_{\kappa'} & \frac{1}{2} & j_{\kappa'}\\ 1 & j_{\kappa_2} & \frac{1}{2}\end{Bmatrix}\begin{Bmatrix}j_{\kappa_1} & 1 & j_\kappa\\ j_{\kappa_2} & 1 & j_{\kappa'}\\ L & 1 & J\end{Bmatrix} . \tag{3.11}$$

$\mathbf{T}_{LJM}(\theta\varphi)$ is a vector spherical harmonic function; it is a simultaneous eigenfunction of orbital angular momentum L, total angular momentum J, and its z projection M. Abbreviation $C^{j\mu}_{j_1\mu_1 j_2\mu_2}\equiv\langle j_1\mu_1 j_2\mu_2|j_1 j_2 j\mu\rangle$ for Clebsch-Gordan (CG) coefficients and usual notations [9] of 6-j and 9-j coefficients are used here. From (3.5)–(3.9) we get the multipole expansion of the current

$$\langle \mathbf{p}\nu|\mathbf{I}(\mathbf{r})|\mathbf{p}'\nu'\rangle=\mathbf{i}\sum_{LJM}I_{LJM}(\mathbf{p}\nu\mathbf{p}'\nu',r)\mathbf{T}_{LJM}(\theta\varphi) , \tag{3.12}$$

with

$$I_{LJM}(\mathbf{p}\nu\mathbf{p}'\nu',r)=\sum_{\kappa\kappa'}Z_{\kappa\kappa' JM}(\mathbf{p}\nu\mathbf{p}'\nu')[X_{LJ}(\kappa\kappa')u^{\epsilon\epsilon'}_{+}(r)+Y_{LJ}(\kappa\kappa')u^{\epsilon\epsilon'}_{-}(r)] \tag{3.13}$$

and

$$Z_{\kappa\kappa' JM}(\mathbf{p}\nu\mathbf{p}'\nu')=\sum_{\mu\mu'}c^{\epsilon}_{\mathbf{p}\nu}(\kappa\mu)^{*}C^{j_{\kappa'}\mu'}_{j_\kappa\mu J M}c^{\epsilon'}_{\mathbf{p}'\nu'}(\kappa'\mu') . \tag{3.14}$$

Substituting (3.12) into the source term of the inhomogeneous field equation, we solve (see Appendix B) the multipole expansion of the color magnetic field

$$\langle \mathbf{p}\nu|\mathbf{H}_s(\mathbf{r})|\mathbf{p}'\nu'\rangle=\sum_{LJM}H_{LJM}(\mathbf{p}\nu\mathbf{p}'\nu',r)\mathbf{T}_{LJM}(\theta\varphi) , \tag{3.15}$$

with

$$H_{LJM}(\mathbf{p}\nu\mathbf{p}'\nu',r)=\begin{cases}-\left[\dfrac{J+1}{2J+1}\right]^{1/2}\displaystyle\int_r^R I_{JJM}(\mathbf{p}\nu\mathbf{p}'\nu',r')r'^{1-J}dr'r^{J-1} & \text{if } L=J-1\ ,\\ -\left[\dfrac{2J+1}{J}\right]^{1/2}\displaystyle\int_r^R I_{J+1JM}(\mathbf{p}\nu\mathbf{p}'\nu',r')r'^{-J}dr'r^{J} & \text{if } L=J\ ,\\ \left[\dfrac{J}{2J+1}\right]^{1/2}\displaystyle\int_0^r I_{JJM}(\mathbf{p}\nu\mathbf{p}'\nu',r')r'^{J+2}dr'r^{-J-2} & \text{if } L=J+1\ .\end{cases} \tag{3.16}$$

The multipole expansion of the sourceless field is (see Appendix B)

$$\langle \mathbf{p}\nu|\mathbf{H}_f(\mathbf{r})|\mathbf{p}'\nu'\rangle=\sum_{JM} b_{JM}(\mathbf{p}\nu\mathbf{p}'\nu')(r/R)^{J-1}\times\mathbf{T}_{J-1JM}(\theta\varphi)\ ; \tag{3.17}$$

the expansion coefficients b_{JM} are determined by the combined boundary condition in the next subsection.

B. Boundary condition and the determination of the color magnetic field

Translational symmetry makes the matrix elements of a field at two corresponding points on opposite windows separated by a basic vector of the Bravias lattice differ only by a factor of absolute value 1. Because the quark wave functions satisfy the periodic boundary condition, the matrix element of the quark current $\langle \mathbf{p}\nu|\mathbf{I}(\mathbf{r})|\mathbf{p}'\nu'\rangle$ and therefore that of the field $\langle \mathbf{p}\nu|\mathbf{H}_s(\mathbf{r})|\mathbf{p}'\nu'\rangle$ directly generated by the current automatically satisfy this condition with the factor $\exp[\mathbf{i}(p_i'-p_i)a_i]$ for $i=1$, 2, and 3. We need only to pose the periodic boundary condition with this same factor on the sourceless field $\mathbf{H}_f$. The MIT boundary condition is $\hat{\mathbf{r}}\times(\mathbf{H}_f+\mathbf{H}_s)=0$ at every point on the wall. The combination of these two conditions is the combined condition, which is a complete boundary condition on the whole surface surrounding the bag cell. It may be written in the form

$$\mathbf{F}(\theta\varphi)-\sum_{JM}\mathbf{G}_{JM}(\theta\varphi)b_{JM}=0 \tag{3.18}$$

for every direction $(\theta\varphi)$, and for every pair $(\mathbf{p}\nu,\mathbf{p}'\nu')$ of quark states. $\mathbf{F}$ and $\mathbf{G}_{JM}$ are vector functions of direction $(\theta\varphi)$.

Multiplying the left-hand side of (3.18) by its Hermite adjoint and integrating the result over 4π solid angle, we obtain a semipositive definite quantity

$$Q=\sum_{JMJ'M'}A_{JM,J'M'}b_{JM}^{*}b_{J'M'}-\sum_{JM}(B_{JM}^{*}b_{JM}+B_{JM}b_{JM}^{*})+C\ , \tag{3.19}$$

with

$$A_{JM,J'M'}=\int_{4\pi}\mathbf{G}_{JM}(\theta\varphi)^{\dagger}\cdot\mathbf{G}_{J'M'}(\theta\varphi)d\Omega\ ,$$
$$B_{JM}=\int_{4\pi}\mathbf{G}_{JM}(\theta\varphi)^{\dagger}\cdot\mathbf{F}(\theta\varphi)d\Omega\ , \tag{3.20}$$
$$C=\int_{4\pi}\mathbf{F}(\theta\varphi)^{\dagger}\cdot\mathbf{F}(\theta\varphi)d\Omega\ .$$

Orthonormality of the set of vector spherical harmonic functions makes us need to do numerical integration only on windows. Q reaches its absolute minimum 0 if and only if condition (3.18) is satisfied. Minimizing Q with respect to b_{JM}^{*}, we obtain

$$\sum_{J'M'}A_{JM,J'M'}b_{J'M'}=B_{JM} \tag{3.21}$$

for all possible JM. A solution of (3.18) must be a solution of (3.21). Therefore, instead of (3.18) we solve the set of equations (3.21). In the numerical calculation, we have to truncate (3.21). It is a truncation of the multipole expansion (3.15) and (3.17) for the color magnetic fields. In these equations only terms with $J\le J_m$ are kept. We put $J_m=15$.

C. Parametrization and integration in the calculation of $E_{\text{c.m.}}$

After having solved the color magnetic fields, we are now going to complete the integrations in (3.4). We complete the volume integration over the bag cell first. The result is a function $E(\mathbf{p},\nu,\mathbf{p}',\nu')$. From the point-group symmetries of the simple cubic lattice we find

$$E(\mathbf{p},\tfrac{1}{2},\mathbf{p}',\tfrac{1}{2})=E(\mathbf{p},-\tfrac{1}{2},\mathbf{p}',-\tfrac{1}{2})=E(0,\mathbf{p},\mathbf{p}')\ ,$$
$$E(\mathbf{p},\tfrac{1}{2},\mathbf{p}',-\tfrac{1}{2})=E(\mathbf{p},-\tfrac{1}{2},\mathbf{p}',\tfrac{1}{2})=E(1,\mathbf{p},\mathbf{p}')\ , \tag{3.22}$$
$$E(k,\mathbf{p}',\mathbf{p})=E(k,\mathbf{p},\mathbf{p}')\ \text{ for } k=0,1\ .$$

To complete the remaining sixfold integration in $\mathbf{p}$ and $\mathbf{p}'$ space, we find an approximate analytic expression for $E(k,\mathbf{p},\mathbf{p}')$. From the symmetry consideration we have found a ten-parameter expression

$$E(k,\mathbf{p},\mathbf{p}')=\sum_{i=0}^{3}\sum_{i'=0}^{3-i}B_{ii'}(k)f_{ii'}(\mathbf{p},\mathbf{p}')\ , \tag{3.23}$$

with

$$f_{ii'}(\mathbf{p},\mathbf{p}')=f_i(\mathbf{p}-\mathbf{p}')[f_{i'}(\mathbf{p})+f_{i'}(\mathbf{p}')]\ . \tag{3.24}$$

For a given $k=|\nu-\nu'|$, we fix ten parameters $B_{ii'}(k)$ in (3.23) by fitting numerically calculated $E(k,\mathbf{p},\mathbf{p}')$ for ten pairs of $\mathbf{p}$ and $\mathbf{p}'$ from four pseudomomenta (0,0,0), $(0,0,\pi/a)$, $(\pi/a,\pi/a,0)$, and $(\pi/a,\pi/a,\pi/a)$. Using (3.23), we reduce the sixfold integration to a few products of threefold integrations in $\mathbf{p}$ space and $\mathbf{p}'$ space separately. We complete these threefold integrations by number theoretical method for numerical integrations [10], which

keeps the numerical error within 2×10^{-3} in limited CPU time. This is necessary for keeping the overall error of energy per nucleon within 2 MeV.

We have also applied this procedure to a spherical MIT bag. In this case everything is analytical. We recovered the expression for the color magnetic energy in [6]. It may be regarded as a check of the procedure.

IV. MODEL PARAMETERS AND NUMERICAL RESULTS

A. Model parameters

To get final numerical results, we need to specify the model parameters. For the MIT bag model, they are the volume energy constant B, the zero-point energy constant z_0, the color fine-structure constant α_c, and the strange-quark mass m_s. Masses for u and d quarks are assumed to be zero. A set of these four parameters has been determined [6] by fitting the hadron spectra. Input masses are those for the nucleon, the Δ isobar, the Ω hyperon, and the ω meson. Baryon mass spectra and ratios between baryon magnetic moments calculated from this set of parameters agree with experiments rather well. The calculated rms charge radius for the proton is slightly smaller than its experimental value. Calculated absolute values of baryon magnetic moments are too small. The situation for mesons is worse. The most serious problem is that of the pion mass. The calculated value is about double that of the experimental value. Although various attempts have been done to escape from this problem, the "disease" is not finally cured.

Having nothing to do with mesons in our MIT bag crystal model for nuclear matter, we concentrate our attention on the baryon sector of bag models. The nucleon structure had been understood in considerable detail by meson-nucleon field theory long before any quark model was proposed. In this theory a physical nucleon is a bare nucleon surrounded by meson clouds. Its radius should therefore be near the Compton wavelength of a π meson, at about 1.4 fm. This point is crucial for getting reasonable results in that theory. In the MIT bag model, there is nothing outside the bag, and the size of the nucleon is about the size of the corresponding bag. In this view, the radius (1 fm) for the nucleon bag calculated from the above set of bag model parameters is too small. The reason of having obtained this set of parameters and therefore the small sizes of baryon bags is that people have tried to fit the meson mass spectra simultaneously. Since this could not be well done, we would rather limit our object to baryons only. In the various chiral bag models, including Skyrmion models, mesons are point particles rather than bags. These bag models are for baryons. They partially recovered the achievements of meson-nucleon field theories on nucleon structure. If the bag is large enough, the pressure of meson clouds on the bag surface may be ignored, and chiral bags approach MIT bags. Therefore we may work with a large MIT bag model for baryons.

Replacing the ω-meson mass by the empirical datum [11] 0.88 fm for the rms charge radius of proton, using the latter and masses of the nucleon, the Δ isobar, and the Ω hyperon as input, we determined a new set of model parameters

$$B^{1/4}=125\ \text{MeV}\ ,\quad z_0=0.88\ ,$$
$$\alpha_c=0.67\ ,\quad m_s=275\ \text{MeV}\ . \tag{4.1}$$

Masses for u and d quarks are assumed to be zero again. The bag radius for a proton corresponding to this set of model parameters increases to 1.207 fm. The calculated absolute value for proton magnetic moment also increases from $1.9\mu_N$ to $2.3\mu_N$, nearer to the experimental value $2.7\mu_N$. Baryon mass spectra calculated from parameters (4.1) are shown in Table I; they are slightly better than the old calculated values quoted from [6].

TABLE I. Baryon masses in unit of MeV.

Baryon	N	Λ	Σ	Ξ	Δ	Σ^*	Ξ^*	Ω
M_{old}	938	1105	1144	1289	1233	1382	1529	1672
M_{new}	939	1110	1157	1301	1233	1383	1530	1672
M_{exp}	939	1116	1193	1318	1233	1385	1533	1672

B. Phenomenological zero point energy for a nonspherical bag

Zero point energies have been calculated from first principles only for a few cases [12]. Even for a spherical MIT bag, it was introduced phenomenologically with a dimensionless constant z_0 determined by fitting experimental data. It seems that, in the present stage, we are only able to extend this phenomenological consideration to general cases. Some general principles may guide us in the extension. The first one is the principle of relativity. This principle tells us that the energy should be deduced from a scalar action. The surface energy may be deduced in this way [13]. This point suggested us to distribute the effective zero point energy on the bag surface. In our model, it is on the wall of the bag cell. The second is the principle of correspondence. This principle tells us that the zero point energy should be characterized by a single dimensionless constant z_0, and should recover the form $-z_0/R$ in [6] for a spherical bag. The simplest form of zero point energy for a static bag fulfilling these conditions is

$$E_0=-z_0\int\frac{(K_g)^{3/2}}{4\pi}ds\ , \tag{4.2}$$

where K_g is the Gauss curvature of the surface at the point under consideration, and the integration is on the surface. For a spherical bag of radius R, $K_g=1/R^2$ [14], we recover the right form $-z_0/R$. For a cut spherical bag cell,

$$E_0=-\frac{z_0}{R}\frac{\Omega}{4\pi}\ , \tag{4.3}$$

where Ω is the total solid angle opened by the wall. In our case, $\Omega=4\pi(3\cos\theta_0-2)$ for a bag cell, and the zero point energy per nucleon is

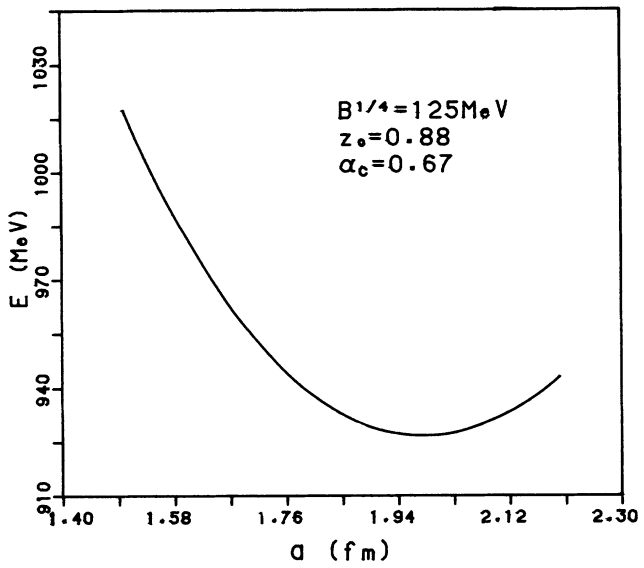

FIG. 3. Average energy per nucleon as a function of lattice constant a in the simple cubic lattice.

$$E_0 = -\frac{z_0}{R}(3\cos\theta_0 - 2) . \tag{4.4}$$

C. Energy per nucleon and nuclear equation of state

According to the MIT bag crystal model considered here, the energy per nucleon E in nuclear matter is a sum of quark energy E_q, color magnetic energy $E_{\text{c.m.}}$, zero point energy E_0, and the volume energy

$$E_v = Bv = \frac{4\pi}{3}R^3(4.5\cos\theta_0 - 1.5\cos^3\theta_0 - 2)B \tag{4.5}$$

per cell. E_q is calculated in Sec. II. Integrations in (3.4) are completed in Sec. III. Substituting the obtained values (4.1) for parameters α_c, z_0, and B in (3.4), (4.4), and (4.5) respectively, we get numerical results for $E_{\text{c.m.}}$, E_0, and E_v, and therefore also for E as a function of a and θ_0. Minimizing E with respect to θ_0 for a given a, we obtain the energy per nucleon $E(a)$ in the ground-state nuclear matter as a function of a, or a function of the nucleon number density a^{-3}, that is, the nuclear equation of state. The numerical function $E(a)$ is shown in Fig. 3. We see a minimum energy per nucleon of $E = 926.4$ MeV at $a = 1.98$ fm; it means a maximum binding energy of 12.6 MeV per nucleon at a saturating nucleon number density of 0.13 fm^{-3}. These results are comparable with corresponding empirical data [15] 15.986 MeV and 0.147 fm^{-3}, and are therefore quite reasonable for a theory in which nothing is adjustable.

V. DISCUSSION

We completed the calculation of energy per nucleon in a MIT bag crystal model for nuclear matter, and derived the nuclear equation of state numerically in this model. In the calculation we considered everything considered previously in the MIT bag model for single hadrons. We are faithful to the MIT bag model in that we have not changed anything in its basic assumptions. What we have added is the lattice geometry. We extended the phenomenological consideration for the zero point energy, but it is a minimum extension consistent with the original idea and general principles. We have reparametrized the model, but it is consistent with the history and the general trend of development for the topic. The color interactions are considered by lowest-order perturbation. This is common in bag models. The overall error in the numerical calculation has been limited to within 2×10^{-3}. It is 2 MeV for energy per nucleon. This is necessary to make the results meaningful.

The main approximation used is the molecular orbit method; it is to use the determinant of the single-quark Bloch states as a zero-order approximate state for the quark system. In this state there is no definite number of quarks in one cell. This is acceptable if the density is not too low, and therefore the energy band is not too narrow. This is the case for the nuclear matter at normal density in our model. When one lowers the density, therefore, bags separate from each other, the windows between bags become smaller, the energy band shrinks, and finally becomes degenerate into a single energy level as shown in [5]. In this case, color interactions, no matter how weak, shall induce a finite configuration mixing, localizing quarks in bag cells, and considerably lowering the energy. We see in Fig. 3 that the energy per-nucleon on the low-density end of the curve is too high, even higher than that for a free nucleon. This is of course unacceptable. The reason for getting this result is that the molecular orbit method fails there. The above-mentioned configuration mixing shall cure this "disease." It may also slightly lower the energy per nucleon around the normal nuclear density. This is in the right direction for improving our result.

We have set the color electric energy to zero. This is justified only in first-order perturbation. In the second-order perturbation, the color polarization is to be considered. There must be a nonzero color electric energy. Since the color fine-structure constant $\alpha_c = 0.67$ is not small enough, the omission of the color electric energy as well as the perturbative treatment of the color magnetic energy is a limitation of the present work. However, this is a limitation of the MIT bag model itself. Every work following this model, including that for single hadrons, shares this limitation. We hope it may be removed in later works.

On the high-density end there is another problem. The geometry of our bag cell (see Fig. 1) makes sense only if $\theta_0 < 45°$. At the normal density the window is already rather wide, $\theta_0 = 42.6°$; at higher density windows will be even wider. There must be a critical density higher than the normal nuclear density, at which a transition of nuclear matter to a new phase occurs. This is a phase of quark gas with normal vacuum bubbles in it; it may be a phase between phases of nuclear matter and of quark-gluon plasma.

We have not considered the motion of the bag as a

whole, for example, the lattice vibration. This is because it becomes less important as the bags open up. It may be considered by quantum bag dynamics [16] in further researches.

We, of course, do not believe that nuclear matter is really a bag crystal. But the reasonable numerical result tells us that perhaps it is not far from the truth. It may be an effective theory if one likes to describe nuclear matter by considering quarks only. Contributions of hadron configuration are averaged and substituted effectively by quark equivalents. This form of theory may be especially suitable for considering the problem of phase transition between nuclear matter and quark-gluon plasma. It offers a quark model for nuclear matter consistent with empirical data and at the same level as bag models for single hadrons, and is therefore better founded for that object.

This work was partly supported by National Science Foundation of China and by the Energy Source Ministry of China.

APPENDIX A: *X* COEFFICIENT AND *Y* COEFFICIENT

We prove expressions (3.10) and (3.11) for X and Y coefficients defined in (3.8) and (3.9), respectively.

Definitions for spinor and vector spherical harmonic functions are

$$\chi_{\kappa\mu}(\theta\varphi)=\sum_{\nu=-1/2}^{1/2} C^{j_\kappa \mu}_{l_\kappa \mu-\nu\,\frac{1}{2}\nu} Y_{l_\kappa \mu-\nu}(\theta\varphi)\chi_\nu \tag{A1}$$

and

$$\mathbf{T}_{LJM}(\theta\varphi)=\sum_{\nu=-1}^{1} C^{J\,M}_{L\,M-\nu\,1\nu} Y_{L\,M-\nu}(\theta\varphi)\mathbf{e}_\nu\ . \tag{A2}$$

$Y_{l\mu}(\theta\varphi)$ is the spherical harmonic function; it is the simultaneous eigenfunction of orbital angular momentum l and its z projection μ. χ_ν is an eigenspinor of z projection ν of spin $\frac{1}{2}$. $\mathbf{e}_\mu$ is an eigenspinor of z projection μ of spin 1, which may be expressed by orthogonal unit vectors $\hat{\mathbf{x}}$, $\hat{\mathbf{y}}$, and $\hat{\mathbf{z}}$ on directions x, y, and z, respectively:

$$\mathbf{e}_{\pm1}=\mp\frac{1}{\sqrt{2}}(\hat{\mathbf{x}}\pm i\hat{\mathbf{y}})\ ,\quad \mathbf{e}_0=\hat{\mathbf{z}}\ . \tag{A3}$$

Using (A1) and the identity

$$Y_{l_1\mu_1}(\theta\varphi)Y_{l_2\mu_2}(\theta\varphi)=\sum_{l=|l_1-l_2|}^{l_1+l_2}\left[\frac{(2l_1+1)(2l_2+1)}{4\pi(2l+1)}\right]^{1/2} C^{l\,0}_{l_1 0\,l_2 0} C^{l\,\mu_1+\mu_2}_{l_1\mu_1\,l_2\mu_2} Y_{l\,\mu_1+\mu_2}(\theta\varphi) \tag{A4}$$

with the orthonormality of CG coefficients and the definition of the 6-j coefficient, we find

$$\begin{aligned}\chi_{\kappa_1\mu_1}(\theta\varphi)^\dagger\chi_{\kappa'\mu'}(\theta\varphi)&=\sum_\mu C^{j_{\kappa_1}\mu_1}_{l_{\kappa_1}\mu_1-\mu\,\frac{1}{2}\mu} C^{j_{\kappa'}\mu'}_{l_{\kappa'}\mu'-\mu\,\frac{1}{2}\mu} Y_{l_{\kappa_1}\mu_1-\mu}(\theta\varphi)^* Y_{l_{\kappa'}\mu'-\mu}(\theta\varphi)\\
&=\sum_{\mu L}(-1)^{\mu_1-\mu}\left[\frac{(2l_{\kappa_1}+1)(2l_{\kappa'}+1)}{4\pi(2L+1)}\right]^{1/2} C^{L\,0}_{l_{\kappa_1}0\,l_{\kappa'}0} C^{j_{\kappa_1}\mu_1}_{l_{\kappa_1}\mu_1-\mu\,\frac{1}{2}\mu} C^{j_{\kappa'}\mu'}_{l_{\kappa'}\mu'-\mu\,\frac{1}{2}\mu} C^{L\,\mu'-\mu_1}_{l_{\kappa_1}\mu-\mu_1\,l_{\kappa'}\mu'-\mu} Y_{L\,\mu'-\mu_1}(\theta\varphi)\\
&=\sum_L(-1)^{\kappa_1}\left[\frac{|\kappa_1|(2l_{\kappa_1}+1)(2l_{\kappa'}+1)}{2\pi}\right]^{1/2} C^{L\,0}_{l_{\kappa_1}0\,l_{\kappa'}0}\begin{Bmatrix} j_{\kappa_1} & l_{\kappa_1} & \frac{1}{2}\\ l_{\kappa'} & j_{\kappa'} & L\end{Bmatrix} C^{j_{\kappa'}\mu'}_{j_{\kappa_1}\mu_1 L\,\mu'-\mu_1} Y_{L\,\mu'-\mu_1}(\theta\varphi)\ .\end{aligned} \tag{A5}$$

Considering also (A2), we obtain

$$\begin{aligned}\chi_{\kappa\mu}(\theta\varphi)^\dagger\hat{\mathbf{r}}\chi_{\kappa'\mu'}(\theta\varphi)&=\sqrt{4\pi/3}\sum_\nu \chi_{\kappa\mu}(\theta\varphi)^\dagger Y_{1\nu}(\theta\varphi)^*\chi_{\kappa'\mu'}(\theta\varphi)\mathbf{e}_\nu\\
&=\sum_{\kappa_1\nu}(-1)^{\kappa_1+l_\kappa+1}\sqrt{2|\kappa|(2l_\kappa+1)}\,C^{l_{\kappa_1}0}_{1\,0\,l_\kappa 0}\begin{Bmatrix} 1 & l_\kappa & l_{\kappa_1}\\ \frac{1}{2} & j_{\kappa_1} & j_\kappa\end{Bmatrix} C^{j_{\kappa_1}\mu+\nu}_{1\nu\,j_\kappa\mu}\,\chi_{\kappa_1\mu+\nu}(\theta\varphi)^\dagger\chi_{\kappa'\mu'}(\theta\varphi)\mathbf{e}_\nu\\
&=\sum_{LJM\kappa_1\nu}(-1)^{l_{\kappa_1}+1}\left[\frac{|\kappa\kappa_1|(2l_\kappa+1)(2l_{\kappa'}+1)(2l_{\kappa_1}+1)}{\pi}\right]^{1/2} C^{l_{\kappa_1}0}_{1\,0\,l_\kappa 0} C^{L\,0}_{l_{\kappa_1}0\,l_{\kappa'}0}\\
&\quad\times\begin{Bmatrix} 1 & l_\kappa & l_{\kappa_1}\\ \frac{1}{2} & j_{\kappa_1} & j_\kappa\end{Bmatrix}\begin{Bmatrix} j_{\kappa_1} & l_{\kappa_1} & \frac{1}{2}\\ l_{\kappa'} & j_{\kappa'} & L\end{Bmatrix} C^{j_{\kappa_1}\nu+\mu}_{1\nu\,j_\kappa\mu} C^{j_{\kappa'}\mu'}_{j_{\kappa_1}\nu+\mu\,L\,\mu'-\mu-\nu} C^{J\,M}_{L\,\mu'-\mu-\nu\,1\nu}\mathbf{T}_{LJM}(\theta\varphi)\ .\end{aligned} \tag{A6}$$

Completing the summation over ν, we get (3.8) and (3.10).

In the same way, defining $\sigma_{\pm 1}=\mp(1/\sqrt{2})(\sigma_x \pm i\sigma_y)$ and $\sigma_0=\sigma_z$, we find

$$\sigma_\nu \chi_{\kappa'\mu'}(\theta\varphi)=\sqrt{3}\sum_{\mu_1} C^{j_{\kappa'}\mu'}_{l_{\kappa'}\mu'-\mu_1\frac{1}{2}\mu_1} C^{\frac{1}{2}\mu_1+\nu}_{\frac{1}{2}\mu_1 1\nu}\chi_{\mu_1+\nu}Y_{l_{\kappa'}\mu'-\mu_1}(\theta\varphi)$$

$$=\sqrt{12|\kappa'|}\,\mathrm{sgn}(\kappa')\sum_{\kappa_1}\delta_{l_{\kappa_1}l_{\kappa'}}\begin{Bmatrix}1 & \frac{1}{2} & \frac{1}{2}\\ l_{\kappa'} & j_{\kappa_1} & j_{\kappa'}\end{Bmatrix} C^{j_{\kappa_1}\mu'+\nu}_{1\nu j_{\kappa'}\mu'}\chi_{\kappa_1\mu'+\nu}(\theta\varphi)\ , \tag{A7}$$

therefore

$$\chi_{\kappa\mu}(\theta\varphi)^\dagger \hat{\mathbf{i}}\mathbf{r}\times\vec{\sigma}\chi_{\kappa'\mu'}(\theta\varphi)=\sqrt{4\pi/3}\,i\sum_{\nu\nu'}(-1)^{\nu'}\chi_{\kappa\mu}(\theta\varphi)^\dagger Y_{1\nu}(\theta\varphi)^*\mathbf{e}_\nu\times\mathbf{e}_{-\nu'}\sigma_{\nu'}\chi_{\kappa'\mu'}(\theta\varphi)$$

$$=\sum_{\nu\nu'\kappa_1\kappa_2}(-1)^{\kappa_1+\kappa_2+l_\kappa+l_{\kappa'}+\nu'}\sqrt{48|\kappa\kappa'|(2l_\kappa+1)}\,\delta_{l_{\kappa_2}l_{\kappa'}}C^{l_{\kappa_1}0}_{10l_\kappa 0}\begin{Bmatrix}1 & l_\kappa & l_{\kappa_1}\\ \frac{1}{2} & j_{\kappa_1} & j_\kappa\end{Bmatrix}$$

$$\times\begin{Bmatrix}l_{\kappa'} & \frac{1}{2} & j_{\kappa'}\\ 1 & j_{\kappa_2} & \frac{1}{2}\end{Bmatrix} C^{j_{\kappa_1}\nu+\mu}_{1\nu j_\kappa\mu}C^{1\nu-\nu'}_{1-\nu' 1\nu}C^{j_{\kappa_2}\mu'+\nu'}_{j_{\kappa'}\mu' 1\nu'}\chi_{\kappa_1\mu_1}(\theta\varphi)^\dagger\chi_{\kappa_2\mu_2}(\theta\varphi)\mathbf{e}_{\nu-\nu'}$$

$$=\sum_{LJM\nu\nu'\kappa_1\kappa_2}(-1)^{l_\kappa+l_{\kappa'}+\kappa_1+\kappa_2+L+J+\mu-1/2}4|\kappa_1\kappa_2|\delta_{l_{\kappa_2}l_{\kappa'}}\left[\frac{3(2l_\kappa+1)(2l_{\kappa'}+1)(2l_{\kappa_1}+1)}{\pi(2L+1)}\right]^{1/2}$$

$$\times C^{l_{\kappa_1}0}_{10l_\kappa 0}C^{L0}_{l_{\kappa_1}0l_{\kappa'}0}\begin{Bmatrix}1 & l_\kappa & l_{\kappa_1}\\ \frac{1}{2} & j_{\kappa_1} & j_\kappa\end{Bmatrix}\begin{Bmatrix}l_{\kappa'} & \frac{1}{2} & j_{\kappa'}\\ 1 & j_{\kappa_2} & \frac{1}{2}\end{Bmatrix}\begin{Bmatrix}j_{\kappa_1} & l_{\kappa_1} & \frac{1}{2}\\ l_{\kappa'} & j_{\kappa_2} & L\end{Bmatrix}$$

$$\times C^{j_\kappa\mu}_{j_{\kappa_1}\mu+\nu 1-\nu}C^{j_{\kappa'}-\mu'}_{j_{\kappa_2}-\mu'-\nu' 1\nu'}C^{1\nu'-\nu}_{1-\nu 1\nu'}C^{L\mu+\nu-\mu'-\nu'}_{j_{\kappa_1}\mu+\nu j_{\kappa_2}-\mu'-\nu'}$$

$$\times C^{J-M}_{L\mu+\nu-\mu'-\nu' 1\nu'-\nu}\mathbf{T}_{LJM}(\theta\varphi)\ . \tag{A8}$$

Completing the summation over ν and ν' by using the definition of 9-j coefficient we obtain (3.9) and (3.11).

APPENDIX B: MULTIPOLE EXPANSION FOR COLOR MAGNETIC FIELDS

From the field equation $\nabla\times\mathbf{H}=\mathbf{I}$, the natural boundary condition $\mathbf{H}_s(\infty)=0$, and the multipole expansion for the current

$$\mathbf{I}(\mathbf{r})=i\sum_{LJM}I_{LJM}(r)\mathbf{T}_{LJM}(\theta\varphi)\ , \tag{B1}$$

we solve the color magnetic field generated by this current in a cut spherical bag of radius R,

$$\mathbf{H}_s(\mathbf{r})=\nabla\times\int\frac{\mathbf{I}(\mathbf{r}')}{4\pi|\mathbf{r}-\mathbf{r}'|}d\tau$$

$$=i\nabla\times\sum_{LJM}\left[\frac{1}{r^{L+1}}\int_0^r I_{LJM}(r')r'^{L+2}dr'+r^L\int_r^R I_{LJM}(r')\frac{dr'}{r'^{L-1}}\right]\frac{\mathbf{T}_{LJM}(\theta\varphi)}{2L+1}\ . \tag{B2}$$

Using the identity

$$\nabla\times[f(r)\mathbf{T}_{LJM}(\theta\varphi)]=\mathbf{i}\times\begin{cases}\left[\dfrac{J+1}{2J+1}\right]^{1/2}\left[\dfrac{df}{dr}-\dfrac{J-1}{r}f(r)\right]\mathbf{T}_{JJM}(\theta\varphi) & \text{if } L=J-1\ , \\ \left[\dfrac{J+1}{2J+1}\right]^{1/2}\left[\dfrac{df}{dr}+\dfrac{J+1}{r}f(r)\right]\mathbf{T}_{J-1JM}(\theta\varphi) & \\ +\left[\dfrac{J}{2J+1}\right]^{1/2}\left[\dfrac{df}{dr}-\dfrac{J}{r}f(r)\right]\mathbf{T}_{J+1JM}(\theta\varphi) & \text{if } L=J\ , \\ \left[\dfrac{J}{2J+1}\right]^{1/2}\left[\dfrac{df}{dr}+\dfrac{J+2}{r}f(r)\right]\mathbf{T}_{JJM}(\theta\varphi) & \text{if } L=J+1\ ,\end{cases} \tag{B3}$$

and the continuity equation $\nabla\cdot\mathbf{I}=0$ for the stationary current $\mathbf{I}$, we get the multipole expansion

$$\mathbf{H}_s(\mathbf{r})=\sum_{LJM}H_{LJM}(r)\mathbf{T}_{LJM}(\theta\varphi)\ , \tag{B4}$$

with

$$H_{LJM}(r)=\begin{cases}-\left[\dfrac{J+1}{2J+1}\right]^{1/2}r^{J-1}\displaystyle\int_r^R I_{JJM}(r')r'^{1-J}dr' & \text{if } L=J-1\ , \\ -\left[\dfrac{2J+1}{J}\right]^{1/2}r^{J}\displaystyle\int_r^R I_{J+1JM}(r')r'^{-J}dr' & \text{if } L=J\ , \\ \left[\dfrac{J}{2J+1}\right]^{1/2}r^{-J-2}\displaystyle\int_0^r I_{JJM}(r')r'^{J+2}dr' & \text{if } L=J+1\ .\end{cases} \tag{B5}$$

The sourceless electric multipole vector potential $r^{J-1}\mathbf{T}_{J-1JM}(\theta\varphi)$ is curlless, therefore only the magnetic multipole vector potential $r^{J}\mathbf{T}_{JJM}(\theta\varphi)$ contributes to the magnetic field. From the identity (B3) we see the multipole expansion for the sourceless magnetic field

$$\mathbf{H}_f(\mathbf{r})=\sum_{JM}b_{JM}\left[\frac{r}{R}\right]^{J-1}\mathbf{T}_{J-1JM}(\theta\varphi)\ . \tag{B6}$$

[1] T. Goldman and G. J. Stephenson, Jr., Phys. Lett. **146B**, 143 (1984).

[2] J. Achtzehnter, W. Scheid, and L. Wilets, Phys. Rev. D **32**, 2414 (1985); M. C. Birse, J. J. Rehr, and L. Wilets, Phys. Rev. C **38**, 359 (1988).

[3] B. Banerjee, N. K. Glendenning, and V. Soni, Phys. Lett. **155B**, 213 (1985); N. K. Glendenning and B. Banerjee, Phys. Rev. C **34**, 1072 (1986).

[4] H. Reinhardt, B. V. Dang, and H. Schulz, Phys. Lett. **159B**, 161 (1985).

[5] Q.-R. Zhang, C. Derreth, A. Schäfer, and W. Greiner, J. Phys. G **12**, L19 (1986).

[6] T. DeGrand, R. L. Jaffe, K. Johnson, and J. Kiskis, Phys. Rev. D **12**, 2060 (1975).

[7] H. Jones, *The Theory of Brillouin Zones and Electronic States in Crystals* (North-Holland, Amsterdam, 1960), p. 89.

[8] E. P. Wigner, *Group Theory* (Academic, New York, 1959), p. 167.

[9] See, for example, A. R. Edmonds, *Angular Momentum in Quantum Mechanics,* 2nd ed. (Princeton University Press, Princeton, New Jersey, 1974).

[10] Hua Loo-Keng and Wang Yuan, *Applications of Number Theory to Numerical Analysis* (Springer-Verlag, Berlin, 1981).

[11] F. Borkowski *et al.*, Nucl. Phys. **A222**, 269 (1975).

[12] G. Plunien, B. Müller, and W. Greiner, Phys. Rep. **134**, 87 (1986).

[13] Q.-R. Zhang, J. Phys. G **14**, 287 (1988).

[14] See, for example, S. Weinberg, *Gravitation and Cosmology* (Wiley, New York, 1972), p. 10.

[15] W. D. Myers and W. J. Swiatecki, Ann. Phys. (N.Y.) **84**, 186 (1974).

[16] Qi-Ren Zhang, Commun. Theor. Phys. **16**, 223 (1991).